ELSEVIER

Journal of Chromatography A, 854 (1999) 245–257

JOURNAL OF CHROMATOGRAPHY A

Characterization of nonyl phenol ethoxylates in sewage treatment plants by combined precursor ion scanning and multiple reaction monitoring

Jeffry B. Plomley[a,*], Patrick W. Crozier[b], Vince Y. Taguchi[b]

[a]*Perkin Elmer–Sciex, 71 Four Valley Drive, Concord, Ontario, Canada L4K 4V8*

[b]*Ontario Ministry of the Environment, 125 Resources Road, Etobicoke, Ontario, Canada M9P 3V6*

Abstract

A novel rapid screening technique for the profiling of nonyl phenol ethoxylates (NPEs) in sewage treatment plant (STP) influent/effluent was developed using flow injection with atmospheric pressure ionization coupled to mass spectrometric analysis by combined precursor ion scanning and multiple reaction monitoring. The technique allows for total NPE concentrations as low as 50 parts-per-trillion to be detected in STP samples.

Keywords: Sewage treatment plants; Mass spectrometry; Nonyl phenol ethoxylates; Ethoxylates; Surfactants

1. Introduction

Nonyl phenol ethoxylates (NPEs) of the form 4–(C_9H_{19})C_6H_4(OCH_2CH_2)$_n$OH, where n=1–16 (NPE–NPE_{16}), are of environmental concern owing to their anaerobic degradation to 4-nonylphenol (NP), a persistent, lipophilic toxicant shown to be a strongly estrogenic compound that has been linked to the feminization of male fish located downstream of sewage treatment plants (STPs) [1,2]. As alkyl aromatic ethoxylated alcohols, NPEs are effective non-ionic surfactants utilized in domestic detergents and cleaners and in the textile and pulp and paper industries. The physical properties of NPEs allow facile transport of this toxicant between non-miscible interfaces such as oil/water, oil/minerals, and water/biological membranes. In 1990, NPE demand in Canada alone was 4.1 kton clearly an impetus for environmental monitoring [3]. However, despite the growing concern of NPEs as precursors of the known endocrine disruptor NP, very few selective and specific analytical techniques exist for its detection in complex matrices, such as those offered by influents and effluents of STPs.

Environmental monitoring of NP and NPEs could be facilitated by a rapid screening technique that would give a presence/absence of total NPEs above/below a specified objective or guideline. Presence above the objective/guideline would result in further speciation of the NPEs. This approach would obviate the need for speciation of samples containing no NPEs or containing NPEs below the objective/guideline.

4-Nonylphenol and lower-molecular-mass NPEs have previously been analyzed utilizing GC–MS techniques [4]. NP is usually derivatized to a less polar molecule [5] although it could be analyzed

*Corresponding author. Fax: +1-905-660-2602.

E-mail address: plomlejb@sciex.com (J.B. Plomley)

0021-9673/99/$ – see front matter
PII: S0021-9673(99)00314-3

underivatized [6]. While investigating the photocatalysis products of NP and NPEs, Sherrard et al. [7] utilized gas chromatography as the only means by which structural isomers of the aliphatic moiety were resolvable. However, the technique was biased towards the lower-molecular-mass NPE homologues due to the poor volatility of higher-molecular-mass NPEs ($>NPE_8$). Consequently, electrospray ionization (ESI) via direct infusion was used in addition to gas chromatography for homologue distribution data; some degree of specificity was achieved using front-end collision-induced dissociation (CID), which furnished $[NPE_4+H]^+$ (m/z 177) as the most predominant product ion. Expectedly, limitations associated with front-end CID were noted by the production of mixed product ion spectra in cocktails of photodegraded surfactant.

Limitations of surfactant volatility in GC–MS analysis can be circumvented by the application of LC techniques. NPEs have been analyzed by either LC–UV [8] or LC–fluorescence [9,10]. Most LC–MS applications of surfactant analysis have been biased towards the chromatographic resolution of linear/branched alcohol ethoxylates or alkyl sulfates, which separate based upon aliphatic chain length on RP supports [11,12]. Under such RP conditions, NPE homologues present in the mixture remain unresolved, such that the ethoxylate distribution must be derived from the extracted ion chromatogram of each molecular ion [13]. However, in the absence of chromatographic separation from matrix species, utilization of only a single stage of MS can result in the adulteration of ethoxylate profiling due to the presence of isobaric interferences. Consequently, a tandem mass spectrometric (MS–MS) technique which offers an inherent degree of selectivity (via precursor ion isolation) and specificity (precursor ion fragmentation to form a product ion spectrum fingerprint) was explored as a means of obviating matrix interference and the need for chromatographic separation. While tandem mass spectrometric techniques often result in a diminution of the absolute signal intensity of the target analyte (relative to single-stage MS), there is a significant improvement in analyte S/N and therefore sensitivity; the improvement in sensitivity is largely conferred by a combination of the selective isolation of a precursor ion from all other species present, as well as the measurement of product ion current derived specifically from an affiliated precursor.

In the development of a continuous flow fast atom bombardment (CF-FAB) MS–MS quantitative procedure for the determination of linear alkylbenzenesulfonates, Borgarding and Hites [14] noted the formation, from all precursors, of a common product ion due to an intact benzenesulfonate moiety. Consequently, triple-stage quadrupole precursor ion scanning was implemented as a selective and specific technique which took advantage of this behaviour. Thus, based upon the investigation of Borgarding and Hites [14], and the observation of an $[NPE_4+H]^+$ common product ion in the front-end CID studies of Sherrard et al. [7], we rationalized that NPEs would exhibit analogous MS–MS behaviour (i.e. production of a common product ion from each NPE precursor ion) conducive to precursor ion scanning. As far as we are aware, there have been no reports detailing the precursor ion scanning tandem mass spectrometric characteristics of NPEs. Therefore, we have investigated such properties and have applied two unique scan functions offered by the triple-stage quadrupole mass spectrometer (i.e. precursor ion scanning and multiple-reaction monitoring, or MRM) in order to develop a rapid flow injection analysis (FIA) technique which profiles ethoxylate distributions in STP samples. Such profiles are invaluable in environmental risk assessment, since NPE toxicity increases with decreasing polyethoxylate chain length [15]. In addition to selective and specific rapid profiling, an MRM semi-quantitative relationship was developed which relates the concentration of total ethoxylate to the summed intensity of each homologue, thereby allowing an estimation of the efficacy with which ethoxylates are eliminated in treated wastewater.

2. Experimental

2.1. General

NPE mass spectral characterization was performed using Igepal CO-210, CO-520, and CO-720 technical mixtures acquired from Aldrich (Milwaukee, WI, USA); three mixtures were required since no single mixture contained all 16 homologues (NPE–NPE_{16})

with sufficient response adequate for instrumental tuning. Increases in Igepal identification number coincide with an increase in average molecular-mass, such that CO-210, CO-520 and CO-720 have associated average molecular-masses of 308, 440 and 749, respectively. Extracted STP samples were prepared by the Ontario Ministry of the Environment (MOE) as follows: a 500 ml aliquot of a 1000 ml water/wastewater sample was acidified to ~pH 2 with 50% sulfuric acid, extracted with dichloromethane (1×80 ml, 2×40 ml), and the extract was dried by passage through anhydrous granular sodium sulfate. The extract was evaporated to dryness, dissolved in 500 μl of methanol, and filtered through a 0.20 μm nylon filter. FIA was automated using a Hewlett-Packard 1100 Series autosampler (20 μl injection volume) and binary pump, the latter operating at either 200 μl/min (ESI) or 600 μl/min (atmospheric pressure chemical ionization, APCI); at these flow rates, FIA run times were <60 s.

2.2. Mass spectrometry

All acquisitions were obtained using a PE-Sciex API 3000 triple quadrupole mass spectrometer (Concord, ON, Canada), operated in a ''mixed loop'' experimental mode, such that two scan events associated with precursor ion scanning, and one scan event detailing 16 MRM transitions could be applied in an alternating fashion in one FIA run. Both Q1 and Q3 mass resolving quadrupoles were operated at unit resolution (~0.7 u at full-width half-maximum). Tandem mass spectra were generated using N_2 target gas, contained in the collision cell at a pressure of ~6 mTorr (1 Torr=133.322 Pa). The electron multiplier was adjusted to give a gain of 10^5 ion counts per second (cps).

2.2.1. Ionization

2.2.1.1. ESI

A 48 ng/μl (total NPE concentration) solution of each Igepal mixture was prepared in 70:30 methanol–water containing 1% acetic acid, and characterized via direct infusion at 10 μl/min into an IonSpray™ Source operated in positive ion mode with an electrospray needle potential of 5.4 kV. FIA required additional desolvation capabilities, as provided by the TurboIonSpray™ source operated at 350°C with a heater gas (N_2) flow rate of 7 l/min.

2.2.1.2. APCI

A 48 ng/μl (total NPE concentration) solution of each Igepal mixture was prepared in acetonitrile–water (30:70) and characterized via split flow infusion (10 μl/min syringe pump+600 μl/min LC pump into a Valco-Tee) at a vaporizer temperature of 450°C, with a nebulization pressure of 75 p.s.i. (N_2), and a needle current of 3.0 μA (1 p.s.i.=6894.76 Pa).

2.2.2. Precursor ion scanning

Precursor ion scanning involved stepping the first mass resolving quadrupole (Q1) over a relevant mass range in defined increments, while the second mass resolving quadrupole (Q3) allowed only one diagnostic fragment ion (generated via CID in Q2) to be transmitted. Consequently, the data from the precursor ion scanning was displayed as a function of the intensity of the specified product ion vs. the mass of the precursor ion from which it was derived. All precursor ion scans were acquired with a dwell time of 2.0 ms per 1.0 u increment, the latter utilizing ''peak hopping'' with an average mass defect for the 16 ethoxylates of 74 mmu/100 u. Q1 was scanned across two mass ranges, 250–400 u and 350–1000 u, coinciding with the detection of precursors of m/z 121 and 133, respectively.

2.2.3. Multiple reaction monitoring

Product ions monitored in precursor ion scanning were also scanned via MRM, resulting in a total of sixteen transitions, each transition monitored for 100 ms and separated by a 5 ms delay time. Optimal collision energy for each dissociative event is presented in Table 1.

3. Results and discussion

3.1. Mass spectral characterization

Fig. 1 represents a Q1 scan for Igepal CO-720; both ESI (a) and APCI (b) data are presented for comparative evaluation. As anticipated, the polymeric distribution was characterized by pseudo-

Table 1
Optimal collision energy for the production of common product ions from NPE precursors NPE–NPE_{16}

$(NPE)_x$ homologue	Precursor $[M+H]^+$	Product ion (m/z)	Optimal collision energy (eV)
1	265	121	24
2	309	121	29
3	353	121	31
4	397	121	35
5	441	133	25
6	485	133	27
7	529	133	29
8	573	133	27
9	617	133	29
10	661	133	31
11	705	133	33
12	749	133	35
13	793	133	40
14	837	133	50
15	881	133	55
16	925	133	55

molecular $[M+H]^+$ ions spaced in 44 u increments, corresponding to differences in the number of $-(CH_2CH_2O)-$ ethoxylate units. In the case of ESI, a second homologous series was noted, likely coinciding to the presence of polyglycol ethers (PGEs) often contained in technical NPE mixtures [16]. Yet a third homologous series was identified as corresponding to Na^+ adduct formation; such sodiation was problematic in that a reduction of ion current for the signal of interest caused a diminution in sensitivity. The problem was exacerbated when the ratio of analyte to Na^+ reached a level where most analyte signal was sodiated. Such sodiation was obviated by APCI; however, low mass NPE homologues were subject to enhanced background noise from impurities present in both the technical mixture (unreacted aliphatic/aromatic alcohols) and mobile phase.

The MS–MS spectra of NPEs were characterized by product ions whose formation resulted from at least two fragmentation streams. In one pathway, product ions retained their aromaticity with the charge located on one of two possible oxygens in the ethoxylate chain (Fig. 2a), giving rise to predominant fragments at m/z 121 and 165. A second dissociative pathway included the formation of product ions of general formula $[NPE_x+H]^+$, resulting from cleavage at two sites in the ethoxylate chain and the neutral loss of nonyl phenol and ethoxylated alcohol (Fig. 2b). The latter pathway furnished abundant product ions at m/z 89, 133, and 177, corresponding to $[NPE_2+H]^+$, $[NPE_3+H]^+$, and $[NPE_4+H]^+$, respectively. NPE homologues NPE and NPE_2 were dominated by product ions at m/z 127 and m/z 183, with m/z 121 being a minor fragment ion. Nonetheless, there was sufficient signal intensity in the m/z 121 transition to allow both NPE and NPE_2 to be detected by MRM in all STP samples analyzed. NPE_3 and NPE_4 both furnished, as the product ion which could be produced in largest abundance, m/z 121. While m/z 121 was also formed by the higher mass homologues, it was not the predominant transition. In fact the propensity for m/z 121 formation decreased as parent mass increased. The opposite trend was noted for the m/z 133 fragment ion $[NPE_3+H]^+$, such that upon increasing parent mass, there was an increase in m/z 133 abundance. Note that m/z 133 represents the product ion which could be formed in largest abundance for NPE_5–NPE_{16}. This is in marked contrast to the source CID results presented by Sherrard et al. [7], where m/z 177 was the predominant fragment ion. The difference in base peak product ion can be attributed to the difference in the centre-of-mass collision energy used to induce fragmentation. We were able to emulate Sherrard's results by reducing collision energy; however, optimal conversion efficiency was realized for the production of m/z 133. Representative product ion spectra in Fig. 3 illustrate the change in base peak product ion as precursor mass increases.

Precursors of m/z 121 and m/z 133, representing ethoxylate homologue ranges of (NPE–NPE_4) and (NPE_5–NPE_{16}), respectively, were optimally detected when ramping collision energy as a function of Q1 mass. Low energy (<100 eV) CID is usually taken as the energy in the laboratory frame (E_{lab}). Conservation of energy and momentum in a collision requires that only a fraction of E_{lab} is available for excitation of the target. This fraction is the centre-of-mass collision energy (E_{cm}), which is inversely related to precursor ion mass (m_p) and directly proportional to E_{lab}, as indicated below:

$$E_{cm} = E_{lab} \times \frac{m_g}{(m_g + m_p)}$$

m_g represent the mass of the target gas. In the case of

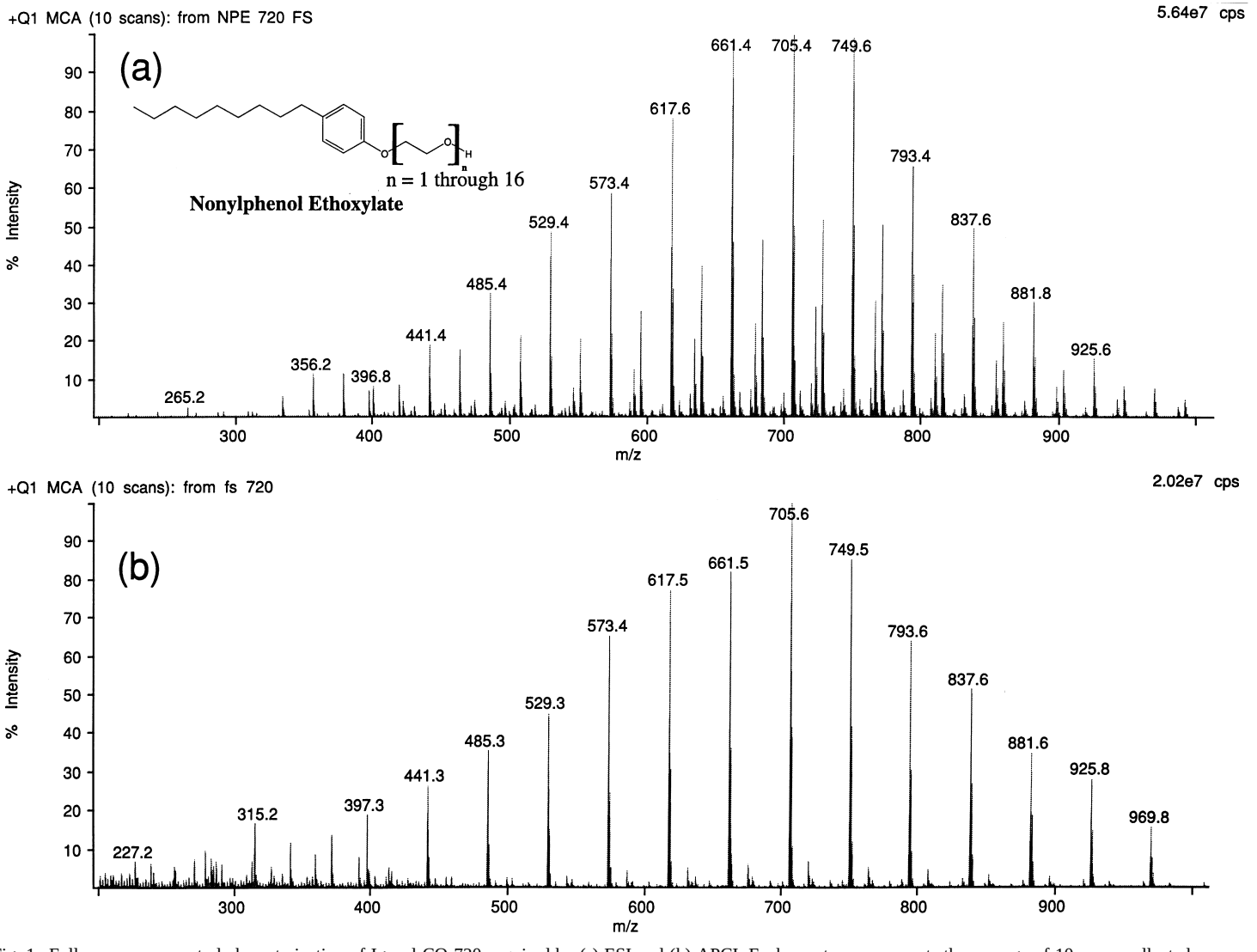

Fig. 1. Full scan mass spectral characterization of Igepal CO-720 acquired by (a) ESI and (b) APCI. Each spectrum represents the average of 10 scans collected over the mass range 200–1000 u in increments of 0.1 u (dwell time: 2.0 ms/u).

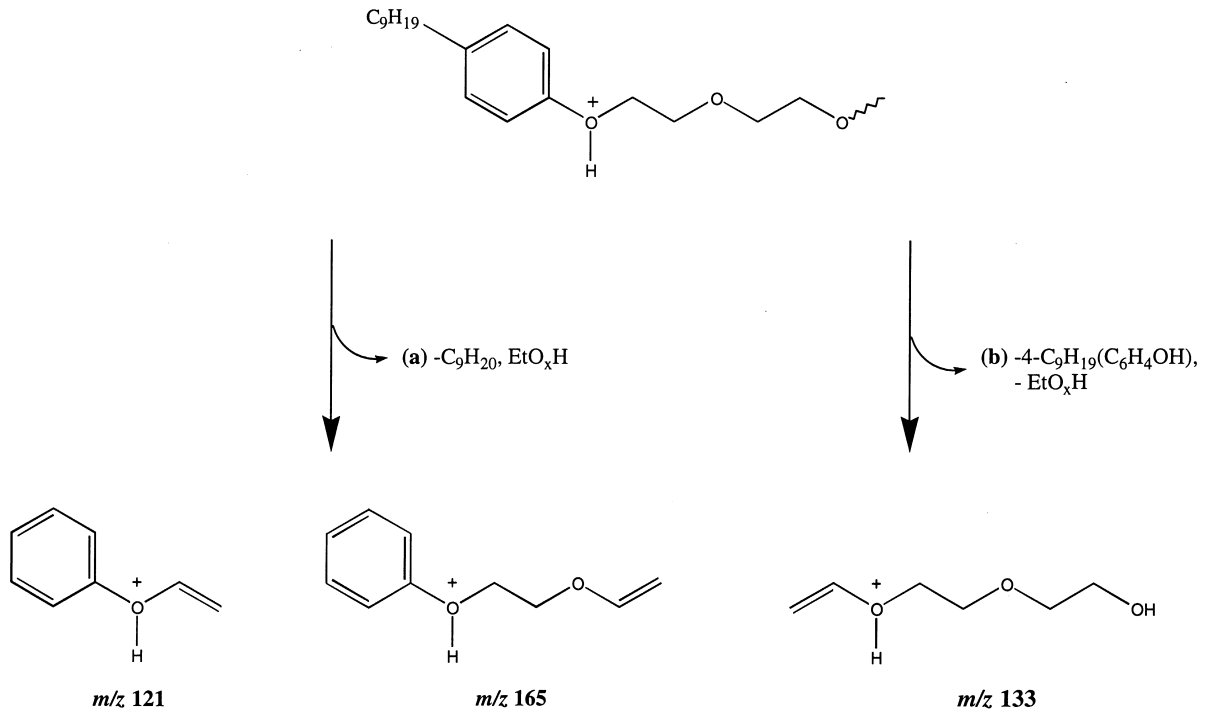

Fig. 2. Proposed fragmentation pathways for the production of (a) m/z 121 and 165, and (b) m/z 133, representative of the formation of product ions of general formula $[NPE_x+H]^+$.

the triple-stage quadrupole, E_{lab} is defined as the axial kinetic energy (i.e. collision energy) of the precursor ion entering the collision cell. If E_{lab} is kept constant, then the centre-of-mass collision energy decreases as a function of increasing precursor ion mass. Consequently, a smaller fraction of kinetic energy is converted to internal energy per collision, such that the conversion efficiency of the dissociative event for the transition of interest decreases (i.e. the absolute intensity of the product ion of interest is reduced). In order to ensure that the relative distribution of homologues in precursor ion scanning mode was identical to that observed by full scan MS, it was thus necessary to ramp collision energy (E_{lab}) as a function of precursor mass in order that E_{cm} be kept relatively constant. Thus, Q1 was scanned from 250 to 400 u for precursors of m/z 121, while concomitantly augmenting collision energy from 22 to 40 eV (note that the phrase 'precursors of m/z 121' is understood to imply 'precursors of product ions having a m/z of 121'). In an analogous fashion, precursors of m/z 133 were detected by scanning Q1 from 350 to 1000 u, while collision energy was ramped from 21 to 58 eV. In order to approximate these collision energy ranges as a function of Q1 scan range, breakdown curves were used to derive the optimal collision energy for each transition of interest (Table 1). Using the collision energy corresponding to the first and last parent mass, the rate of change in collision energy as a function of ethoxylate mass was then calculated and applied to the appropriate Q1 scan range. Consequently, the homologue distribution obtained by precursor ion scanning (Fig. 4) closely emulated the envelope acquired in a Q1 scan (Fig. 1b). This eliminated any discrimination in precursor signal intensity which could result if a fixed collision energy were defined.

The analysis of NPEs in STP samples revealed some limitations associated with precursor ion scanning as a stand-alone technique when coupled with ESI. As noted in Fig. 5a,b for an STP effluent sample, NPE–NPE_8 were delineated in a precursor ion scanning mode from other ionizable species in

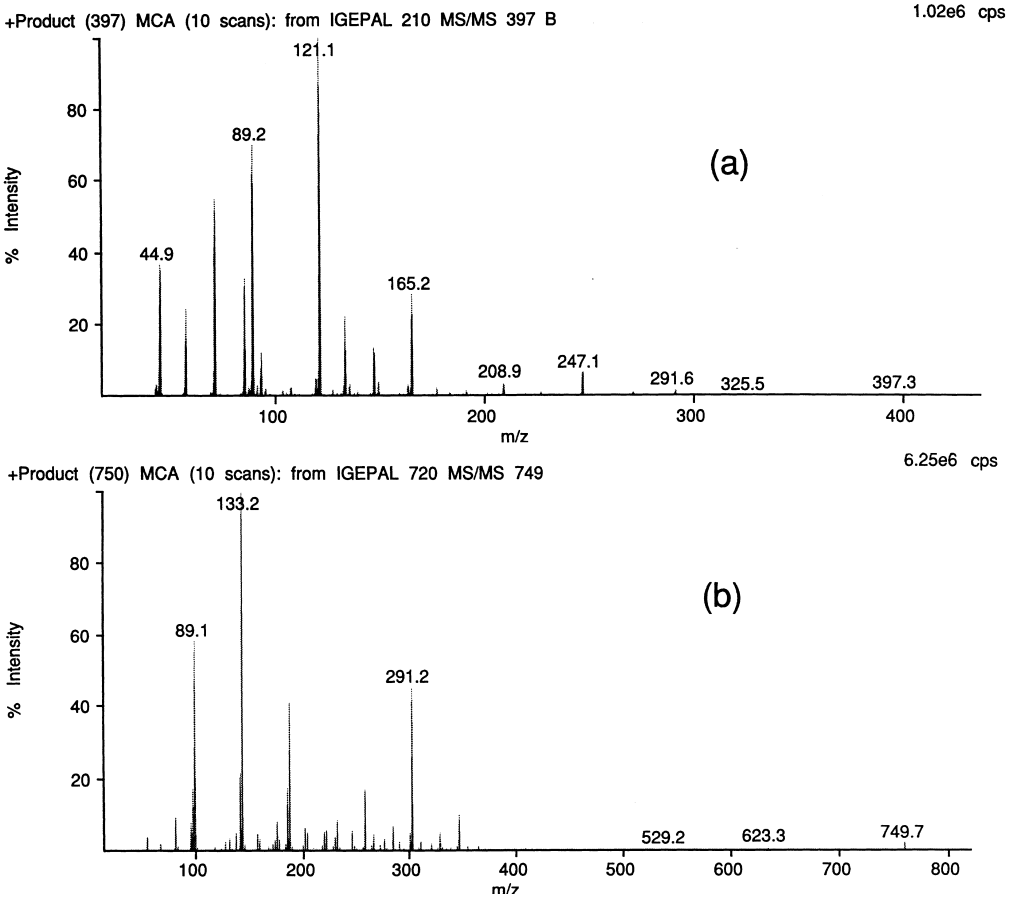

Fig. 3. Change in relative abundance of m/z 121 and 133 as a function of precursor mass for (a) NPE_4 and (b) NPE_{12}.

the background. However, due to poor analyte response and the presence of a signal at virtually every Q1 mass scanned, it was difficult to extract homologues $>NPE_8$. Consequently, MRM of the sixteen homologues (Table 1) were looped with the two precursor ion scanning events in order to obtain a cleaner 'extraction' (and thus more rapid visual profiling) for only those species of interest. Additionally, MRM provided an enhancement in sensitivity. As indicated in Fig. 5c, the MRM envelope closely approximated the relative abundance of those precursor ions detected by precursor ion scanning. As well, MRM adequately profiled homologues $>NPE_8$. Note that the product ions used in MRM were identical to those in precursor ion scanning. Although transitions different than those monitored in precursor ion scanning could have been applied in MRM as confirmatory ions, it was necessary for the MRM analyte distribution to emulate the precursor ion scan envelope. This envelope in turn emulates the Q1 distribution and is thus representative of the nominal NPE_x value. Arguably, MRM alone would suffice as a stand-alone technique for NPE profiling. However, precursor ion scanning offers additional information regarding STP constituents which are related to NPEs, and thus is useful for characterizing the efficacy of wastewater treatment (see below) for the removal of NPEs.

In marked contrast to the STP effluent precursor ion scan profile obtained by ESI, the APCI derived precursor ion scan spectra (Fig. 6a and b) furnished an enhanced analyte S/N ratio, such that virtually all homologues were clearly defined. The tendency of ES to ionize a broader range of background species

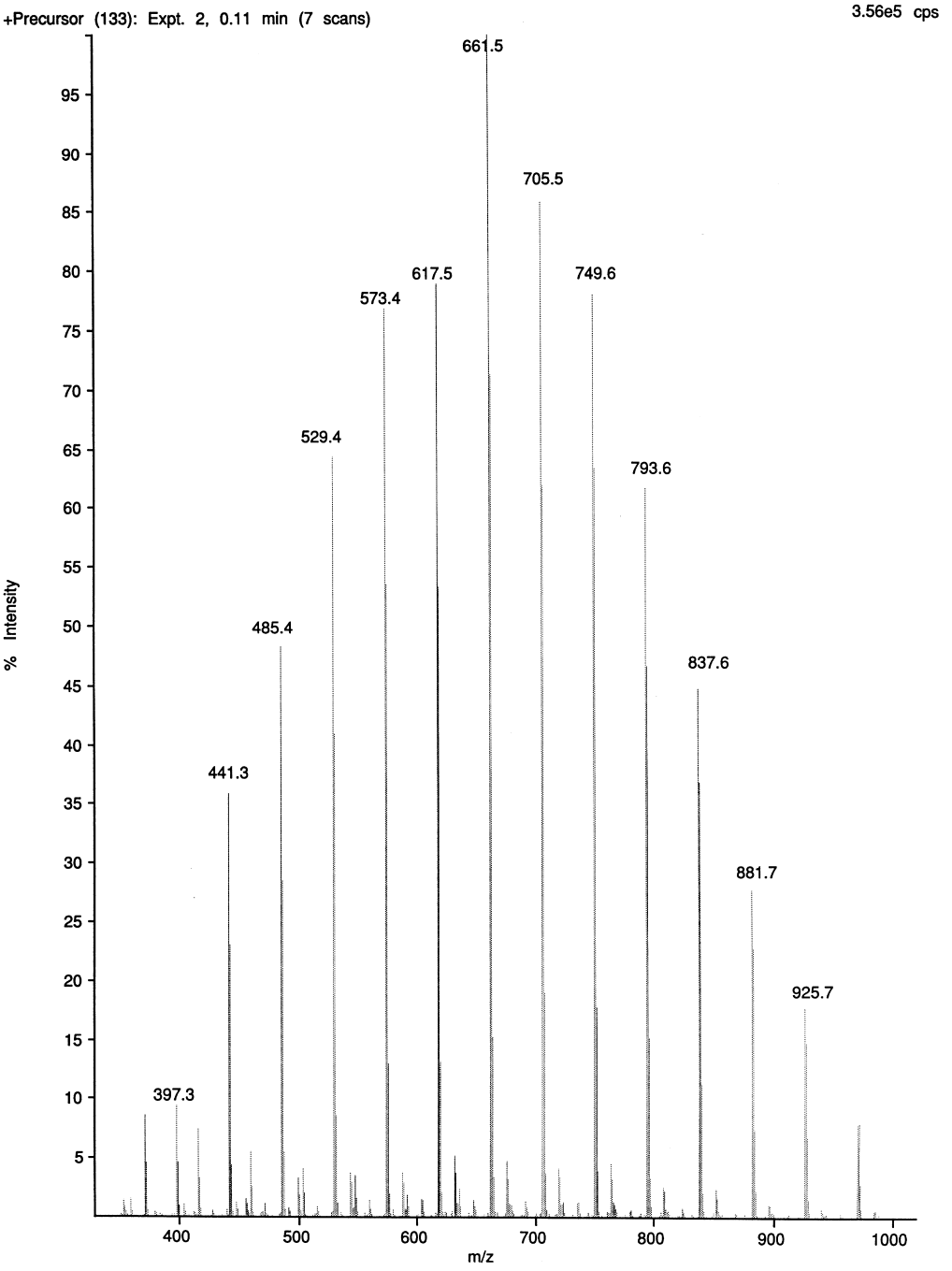

Fig. 4. Scanning precursors of m/z 133 from Igepal CO-720 while ramping collision energy from 21–58 eV demonstrating the maintained integrity of the Q1 distribution (nominal NPE_x value).

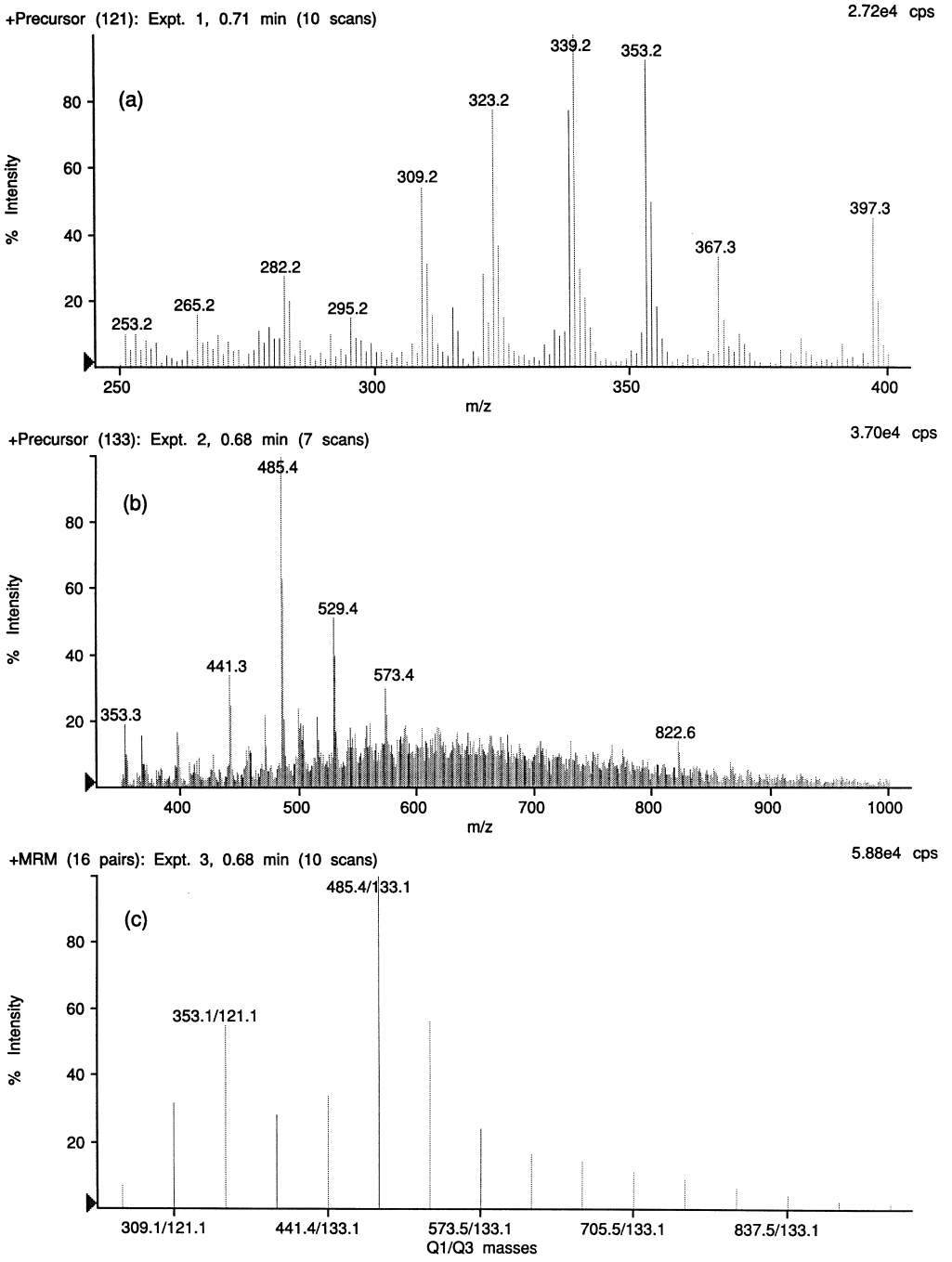

Fig. 5. ESI analysis of STP effluent by looped experiments for (a) precursors of m/z 121, (b) precursors of m/z 133, and (c) product ions resulting from 16 individual MRM transitions.

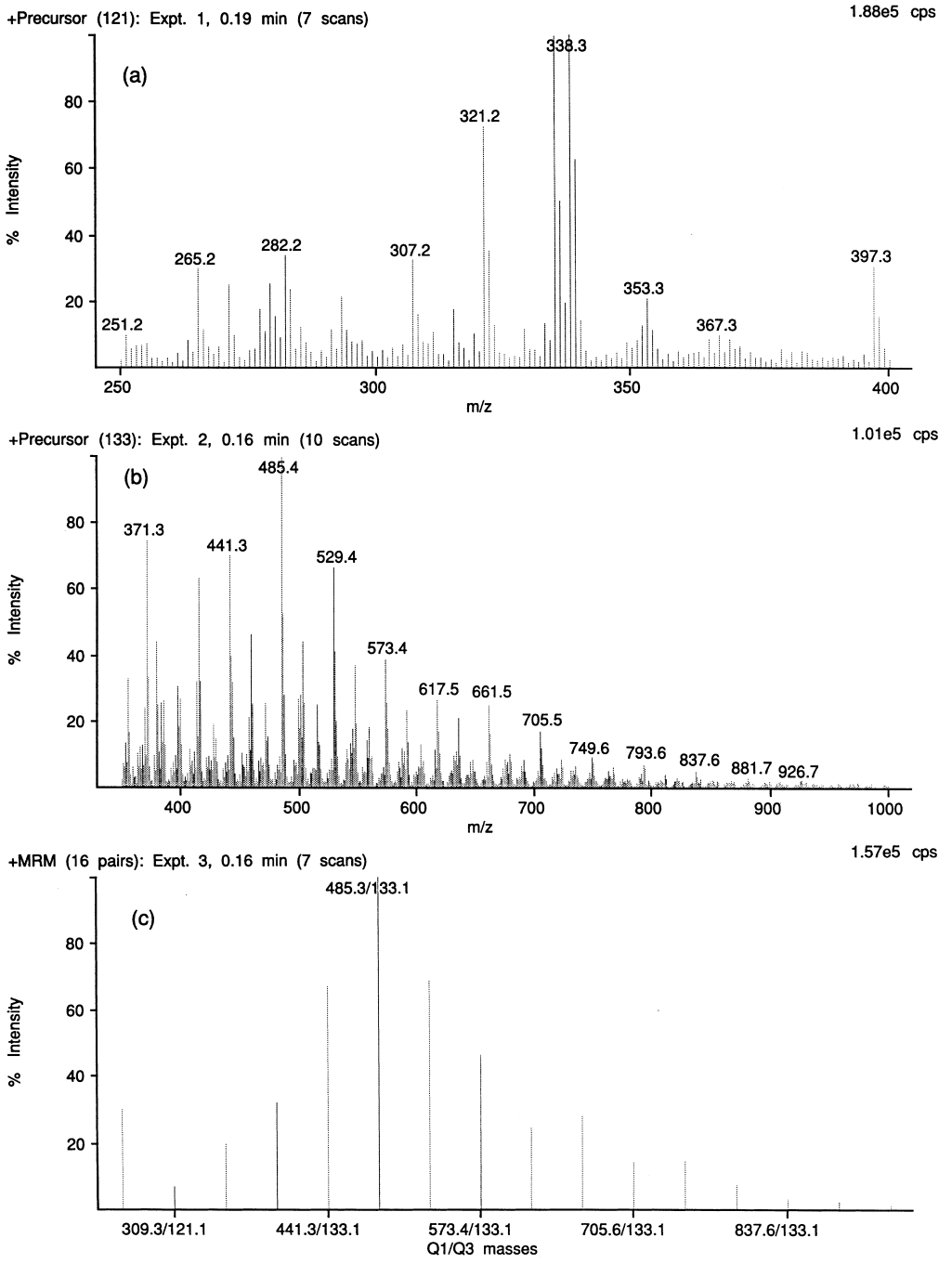

Fig. 6. APCI analysis of STP effluent by looped experiments for (a) precursors of m/z 121, (b) precursors of m/z 133, and (c) product ions resulting from 16 individual MRM transitions. Note the enhanced S/N in (b) relative to that shown in Fig. 5b for ESI. A nominal NPE_x value of 6 may be ascertained from the MRM data.

(thereby reducing S/N for the less abundant homologues) was noted for most STP samples analyzed. Thus, in the absence of chromatography, APCI appeared to be the ionization mode of choice for the STP matrix, not only for NPEs, but other components as well. For example, other homologous series were detected, and may represent a combination of polyglycol ethers (PGEs) and carboxylated NPEs (CNPEs) [16], the latter reported as degradation products of NPEs [17].

A further benefit of APCI over ES may be derived from the fact that many reported NPE separations are based upon structural differences related to the number of ethoxylate subunits from which a homologue is constructed [12,18–20]. As such, normal-phase HPLC techniques are utilized for which APCI is inherently better suited than ES. Furthermore, NPEs may be efficiently extracted from STPs using dichloromethane, a common component in mobile phase compositions used to separate NPEs [12].

The rapid profiling of NPE distribution by FIA/APCI/precursor ion scanning/MRM is a particularly powerful and rapid analytical technique for gauging the efficacy with which such species are removed from STP influents. For example, Fig. 7a–c represents the NPE profile for the STP influent corresponding to the STP effluent. Clearly, the untreated wastewater shows a larger number of constituents other than NPEs which give rise to precursors of m/z 133, most of which are spaced in 44 u increments, and thus represent a homologous series likely attributed to a mixture of PGEs, CNPEs, and linear alcohol ethoxylates. Furthermore, the MRM data indicate that the influent is characterized by a greater abundance of high-molecular-mass NPE homologues (nominal NPE_x value of 10). Upon initial inspection, Fig. 6c (MRM of the 'treated' wastewater) indicates that the degree of nonyl phenol ethoxylation has apparently shifted to the lower (and more toxic) homologues (nominal NPE_x value of 6), while the precursor ion scan data in Fig. 6b shows a reduction in the unidentified constituents detected in the influent, indicating that some adulteration has occurred. A graphical representation of the absolute MRM signal intensity for each homologue (Fig. 8) in both the influent (first bar) and effluent (second bar) reveals that the wastewater 'treatment' was effective only for the removal of ethoxylates NPE_5 to NPE_{16}; the signal intensity of the lower homologues NPE–NPE_4 actually show an increase in the effluent sample. This latter result was corroborated by quantitative GC–MS, such that total NPE concentrations of 1 ng/mL and 8 ng/mL were reported for the influent and effluent, respectively. It should be recognized that the GC–MS results are biased towards NPE–NPE_7 homologues at the concentrations detected. It is clear that this particular treatment plant reduced but did not completely eliminate (at the time of sample collection) all NPEs entering the treatment centre. Furthermore, the treatment exercised by the plant was biased towards a reduction only in the higher NPE homologues.

In order to establish a semi-quantitative approach to influent/effluent NPE flux, the summed signal intensity of NPE–NPE_{16} derived from MRM was plotted as a function of total mass of ethoxylate injected, over the range 1.00–1000 ng. Parenthetically, 1.00 ng of total NPE injected corresponds to <60 pg per ethoxylate homologue detected. A four point linear regression forced through zero resulted in a correlation coefficient of 0.99976 with a slope of 2.999 and a standard error of ± 0.006061. Each calibration point was the average intensity of three replicate injections. Application of the calibration plot for components detected in STP samples relied upon all homologues being present. Clearly, estimation of the concentration of total ethoxylates contained in a sample becomes progressively worse as the number of detectable homologues decreases. Fortunately, the limited number of samples we analyzed in the current investigation had all 16 ethoxylates present, albeit in different relative abundance from the Igepal CO-720 used to construct the calibration curve. However, because we were only interested in the *relative* adulteration of NPEs in the treatment process, the current methodology has merit as a semi-quantitative approach to NPE flux. Thus, calculation of the total NPE concentration in the STP effluent and the STP influent revealed that some 37 μg/mL (78%) of total NPE was removed by the STP. Coupled with the calculations presented graphically in Fig. 8, it can be concluded that the 78% reduction in total NPEs was due to the preferential removal of NPE_5–NPE_{16}. It should be noted that based upon the instrumental detection limit (i.e. 1.00 ng) and the sample preparation scheme, this current

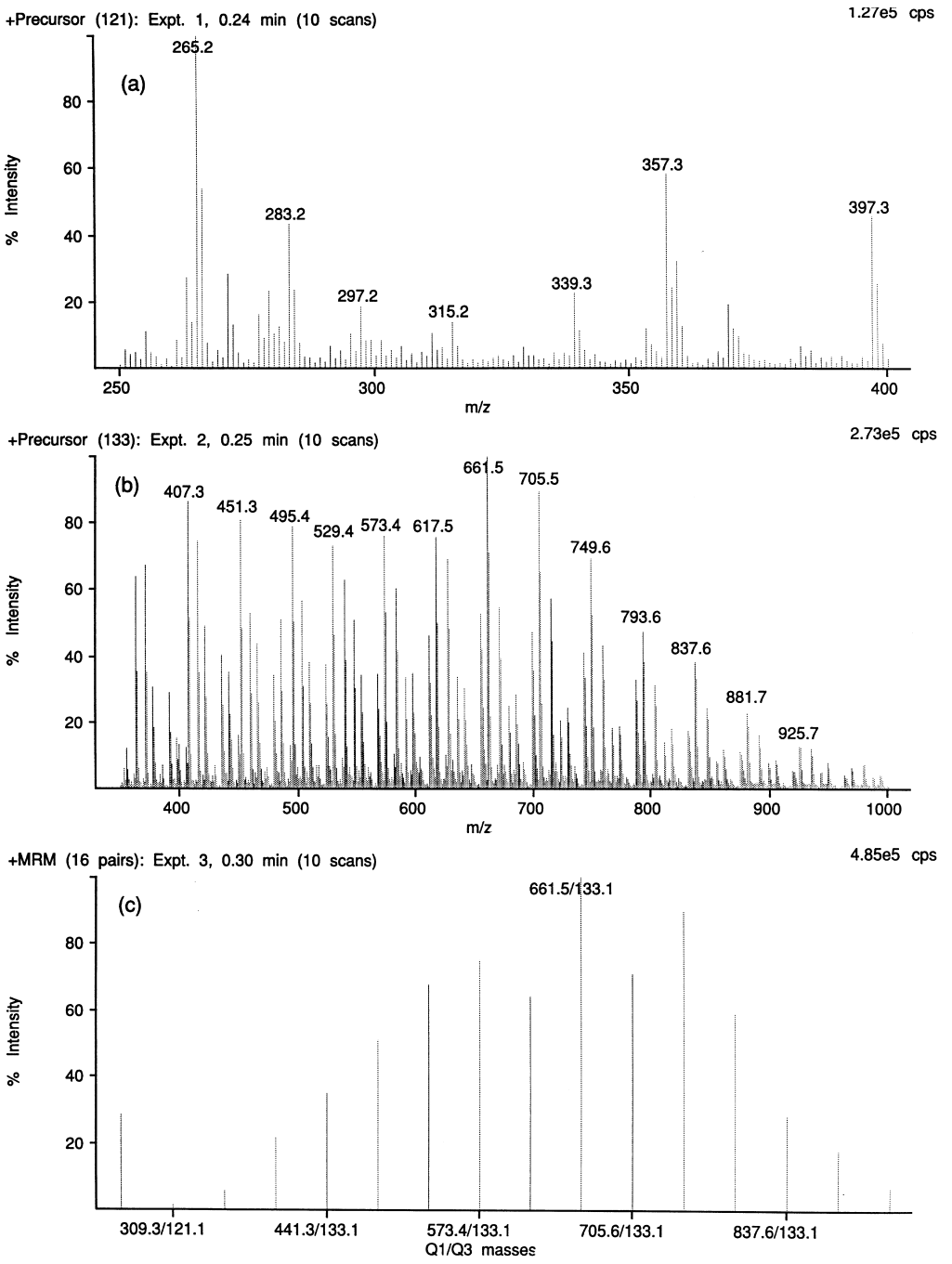

Fig. 7. APCI analysis of STP influent by looped experiments for (a) precursors of m/z 121, (b) precursors of m/z 133, and (c) product ions resulting from 16 individual MRM transitions, demonstrating a nominal NPE_x value of 10.

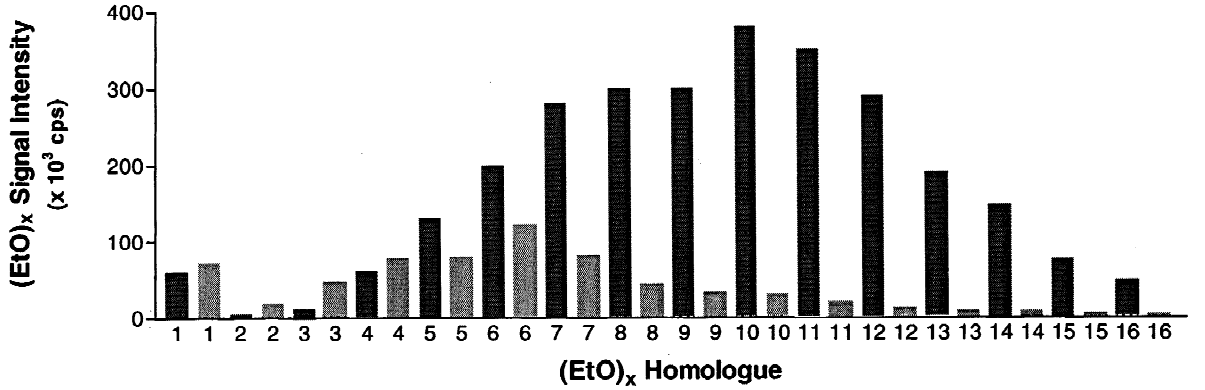

Fig. 8. NPE_x absolute signal intensity for each NPE homologue detected in STP influent (first bar) and effluent (second bar) by APCI/MRM.

screening technique is capable of detecting ~50 ppt of total NPEs in STPs.

4. Conclusions

Although a preliminary investigation, the above results suggest that the combination of APCI and triple-stage quadrupole mass spectrometry, with the selectivity and specificity of combined precursor ion scanning and MRM, offers a significant improvement over current methodologies for the detection and characterization of NPE profiles. Future endeavors include the tandem mass spectral characterization of PGEs, CNPEs and linear alcohol ethoxylates, all suspected to be present in the STP samples analyzed. As well, the development of a more rigid quantitative procedure is currently in progress. A reversed-phase LC system was developed to separate classes of surfactants. Because the structural difference and overall polarity of NPE homologues are dictated by the number of ethoxylate subunits, a normal-phase LC system was also developed to provide adequate separation such that, when coupled to MRM, a quantitative procedure based upon integrated peak area and isotopic dilution can be realized.

References

[1] E. Pelizzetti, C. Minero, V. Maurino, A. Sclafani, H. Hidaka, N. Serpone, Environ. Sci. Technol. 23 (1989) 1380.
[2] A.M. Soto, H. Justicia, J.W. Wray, C. Sonnenschein, Environ. Health Persp. 92 (1991) 167.
[3] Nonylphenol Ethoxylates-Reduction and Phase-Out Initiatives, World Wildlife Federation (WWF) Canada Report, Ottawa, 1997.
[4] N. Kannan, N. Yamashita, G. Petrick, J. Duinker, Environ. Sci. Technol. 32 (1998) 1747.
[5] H. B. Lee, T.E. Peart, Anal. Chem. 34 (1995) 1976.
[6] P. deVoogt, K. de Beer, F. van der Wielen, Trends in Anal. Chem. 16 (1997) 584.
[7] K.B. Sherrard, P.J. Marriott, R.G. Amiet, M.J. McCormick, R. Colton, K. Millington, Chemosphere 33 (1996) 1921.
[8] K. Fyianos, S. Pegiadou, N. Raikos, I. Eleftheriadis, H. Tsoukali, Chemosphere 35 (1997) 1423.
[9] H. B. Lee, T.E. Peart, Water Qual. Res. J. Canada 33 (1998) 389.
[10] L.G. Mackay, M.Y. Croft, D.S. Selby, R.J. Wells, J. AOAC Int. 80 (1997) 401.
[11] A. Di Corcia, J. Chromatogr. A 794 (1998) 165.
[12] P. Jandera, M. Holcapek, G. Theodoridis, J. Chromatogr. A 813 (1998) 299.
[13] C. Crescenzi, A. DiCorcia, R. Samperi, A. Marcomini, Anal. Chem. 67 (1995) 1797.
[14] A. Borgarding, R.A. Hites, in: Proceedings of the 39th ASMS Conference on Mass Spectrometry and Allied Topics, Nashville, TN, 1991, p. 714.
[15] R.D. Swisher, Surfactant Biodegradation, 2nd ed, Marcel Dekker, New York, 1987.
[16] E.T. Furlong, P.M. Gates, in: Proceedings of the 45th ASMS Conference on Mass Spectrometry and Allied Topics, Palm Springs, CA, 1997, p. 942.
[17] M. Ahel, T. Conrad, W. Giger, Environ. Sci. Technol. 21 (1987) 697.
[18] I. Zeman, J. Chromatogr. 363 (1986) 223.
[19] R.E. Murphy, M.R. Schure, Anal. Chem. 70 (1998) 4353.
[20] H.B. Lee, T.E. Peart, D.T. Bennie, R.J. Maguire, J. Chromatogr. A 785 (1997) 385.